Low-frequency dynamics in an optical strong glass: vibrational and relaxational contributions

1997 J. Phys.: Condens. Matter 9 3955

(http://iopscience.iop.org/0953-8984/9/19/015)

J. Phys.: Condens. Matter **9** (1997) 3955–3971. Printed in the UK PII: S0953-8984(97)77978-5

Low-frequency dynamics in an optical strong glass: vibrational and relaxational contributions

F Terki, C Levelut, J L Prat, M Boissier and J Pelous

Laboratoire des Verres, UMR 5587, Université Montpellier II, Place Eugène Bataillon, Case 069, 34095 Montpellier Cedéx, France

Received 19 September 1996, in final form 3 February 1997

Abstract. A detailed Raman and Brillouin scattering investigation on a strong glass over a wide range of temperature across the glass transition temperature T_g is presented. The aim of the study is to determine whether the low-frequency vibrational behaviour is correlated with the elastic properties. A careful comparison of several models is carried out in order to determine the reliability of theoretical predictions devoted to the understanding of the dynamics of glass-forming systems. A clear correlation between the position of the boson peak and the hypersonic velocity in both polarizations is demonstrated; in particular, the connection is in better accordance if one considers the transverse velocity. On the other hand, the quasielastic Raman scattering has been analysed in terms of excitations directly coupled to the acoustic phonons. The correlation between the quasielastic Raman intensity and the hypersonic attenuation predicted for the low-temperature regime has been found to hold over a broad range below and above T_g. We found a strong correlation between the Raman features (at 10–50 cm^{-1}) and the Brillouin data (at 1 cm^{-1}), suggesting that the same mechanism is responsible for the vibrational dynamics within the 1–50 cm^{-1} range. Moreover, we emphasize that the softening of the vibrational modes responsible for the boson peak occurs significantly below T_g, while an increase of the quasielastic intensity sets in, indicating some similarity between the origin of the boson peak and the origin of the growth of the quasielastic line.

1. Introduction

The dynamics of the glass transition has been extensively studied within the last decade. Many discussions focus on the relaxational processes and their temperature dependence across the liquid–glass transition. New steps in the investigations were stimulated by the achievement of the so-called mode-coupling theory (MCT) [1, 2]. The MCT introduces two relaxational processes for a single variable: a slow (α-) relaxation with a strong temperature dependence, and a fast (β-) relaxation varying slowly with the temperature. A quantitative agreement of the predictions of this theory is obtained for fragile (in Angell's classification [3]) glasses and a qualitative one for intermediate glasses. The relaxational contribution appears as the quasielastic line dominating the spectra at lower frequencies (below 10 $cm^{-1} \equiv 0.3$ THz), especially above the glass transition temperature T_g. This contribution exhibits a very strong temperature dependence.

Nevertheless, in the frequency range of the fast relaxation, a significant part of the dynamic structure factor is due to low-energy vibrations. These vibrational excitations appear as an excess in the density of states at around 20–50 $cm^{-1} \equiv 0.6$–1.5 THz in both inelastic neutron and Raman scattering data as the so-called boson peak (BP), which is the

0953-8984/97/193955+17$19.50

dominating feature at low temperature. The intensity of the BP varies with temperature like the Bose factor $(n(\omega, T) + 1)$.

The vibrational part is not taken into account in the MCT. The increase of this contribution, when going from fragile toward strong glass-formers [4], is responsible for a quantitative discrepancy between the predictions of the MCT and the experimental results for strong glass-formers [5]. This vibrational contribution has to be taken into account in the analysis of the Raman and neutron data. Several models attempted to consider both relaxational and vibrational contributions [6, 7]. One of them introduces a strong coupling between these two kinds of contribution. The authors assume that the vibrational excitations seen as the BP at $T \ll T_g$ are coupled to some relaxing variable which does not itself contribute to the scattering but induces a broadening of each frequency of the BP [6]. Another model suggests a transformation from vibrational modes to relaxational ones [7]. The 'vibration–relaxation' model developed by Buchenau for the interpretation of neutron scattering data for polymers [7, 8] suggests a transformation from vibrational modes to relaxational ones. It introduces a crossover from more or less damped vibrations at high frequencies to low-barrier relaxations at low frequencies. This model is a simplified classical version of the soft-potential model for glasses [9, 10]. It predicts that high-frequency (above the BP) modes are vibrational ones: two thirds coming from eigenmodes corresponding to positive eigenvalues which stay vibrational at lower frequencies, and one third corresponding to negative eigenvalues. The modes with negative eigenvalues move in a double-well potential and can turn into a relaxational contribution at low frequency by jumping over the barrier.

Several models have been proposed for the interpretation of the maximum related to the vibrational density of states $g(\omega)$ responsible for this peak (the maximum occurs in $g(\omega)/\omega^2$). Some authors associated the BP with a characteristic frequency of clusters with sizes in the 10–20 Å range [11–13]. Other models attributed the maximum to the localization of the phonons by disorder through a mechanism of phonon scattering by density fluctuations or by coupling with low-energy excitations [14–17]. Most of these models associate the position of the BP with a correlation length [18, 19] defined as $\ell \propto V/\omega_{max}$ where V is the velocity of sound and ω_{max} the position of the maximum of the BP. ℓ may be identified with a cluster size (ω_{max} being a vibrational frequency of the cluster), or with a correlation length over which short-range order and medium-range order are maintained [14]. In the models where the BP occurs due to localization of the phonons [14, 17], ℓ has the meaning of a localization length in the Ioffe–Regel definition. This characteristic length has often been reported to be constant as temperature is varied [19–21]. A temperature-independent ℓ-value means that the position of the BP is correlated with the velocity of sound.

On the other hand, several models suggest a connection between the Raman-reduced intensity $I_R(\omega, T)$ and the hypersonic attenuation $\alpha(\omega, T)$, such as $I_R(\omega, T) \propto \alpha(\omega, T)(1+n(\omega, T))/\omega$, underlying a common origin for these two physical properties in the low-temperature range. This correlation was first proposed by Theodorakopoulos and Jäckle [22, 23] in the case of silica, where defects which can have two distinct states of polarizability are responsible for a quasielastic intensity due to the relaxation of these defects as well as the hypersonic attenuation in the GHz range: then, the relaxational Raman scattering excess I^{rel} and the hypersonic attenuation α^{rel} of relaxational origin are proportional. In the framework of the soft-potential model, Gurevich *et al* [24, 25] have established this connection, and discussed the temperature and frequency dependence of these quantities. They showed that the proportionality relationship affects the total Raman scattering [24, 25]. Moreover, Buchenau *et al* gave evidence for such similarities in the temperature dependence between the Raman intensity (or the inelastic neutron scattering

data) and the ultrasonic or infrared attenuations for temperatures below 300 K in silica [26]. These results support the hypothesis of a common origin on the basis of classical activated relaxation processes. In this study, we will demonstrate that it is possible to extend the previous prediction to the high-temperature regime.

Here, we present a Brillouin and low-frequency Raman scattering investigation on a strong glass-former performed across the glass transition temperature. The measurements have been carried out to test, over the whole temperature range, the connection between:

(i) the maximum of the BP and the hypersound velocity on the one hand; and
(ii) the relaxational reduced Raman intensity and the hypersonic attenuation on the other hand.

For this purpose several models have been used to extract the vibrational and relaxational contributions.

2. Measurements

Brillouin and Raman scattering experiments were performed on a BAF4 glass over a wide temperature range using the same experimental set-up as described in [30]. This sample is a commercial optical glass provided by Schott, and its glass transition temperature is equal to 796 K.

The Brillouin scattering measurements of transverse and longitudinal sound velocities at hypersonic frequencies were performed from room temperature to 1200 K in an oven fitted with optical windows. The regulation of the temperature was a conventional PID regulation. The temperature was measured a few millimetres from the sample using a platinum/platinum–rhodium alloy (S) thermocouple. The sample was contained in a silica cell of optical quality. The accuracy of the experimental data for the velocity of sound and the attenuation was of about 0.1% and 5% respectively. As the transverse signal was lower than the longitudinal one, the transverse velocity of sound became more difficult to determine at temperatures where the sample became opalescent and therefore yielded an increase in the elastically scattered intensity. Thus, the accuracies for the transverse velocity and attenuation were about 1% and 10% respectively.

Stokes and anti-Stokes Raman spectra were measured in right-angle geometry from room temperature to 1020 K in the same oven as the one for Brillouin measurements and from 10 K to room temperature in a helium cryostat. The Raman spectra were recorded in the vertical–horizontal (VH) polarization in the 5–1500 cm^{-1} frequency range.

3. Results and data analysis

3.1. Brillouin results

The position $\delta\nu$ and the half-width at half-maximum Γ of the Brillouin line were determined using a fitting procedure in which the convolution of a Lorentzian function with the experimentally determined apparatus function was adjusted to the spectra. The hypersound transverse and longitudinal velocities V as well as the attenuation α were calculated like in [30]. The temperature dependence of the refractive index, usually weak in glasses, has been neglected. It has been shown in a previous study that the strongest effect on the refractive index is around the glass transition [27, 28] where its absolute variation is less than 10^{-2} in most glasses [29], leading to variations of less than 1% for the velocity of sound.

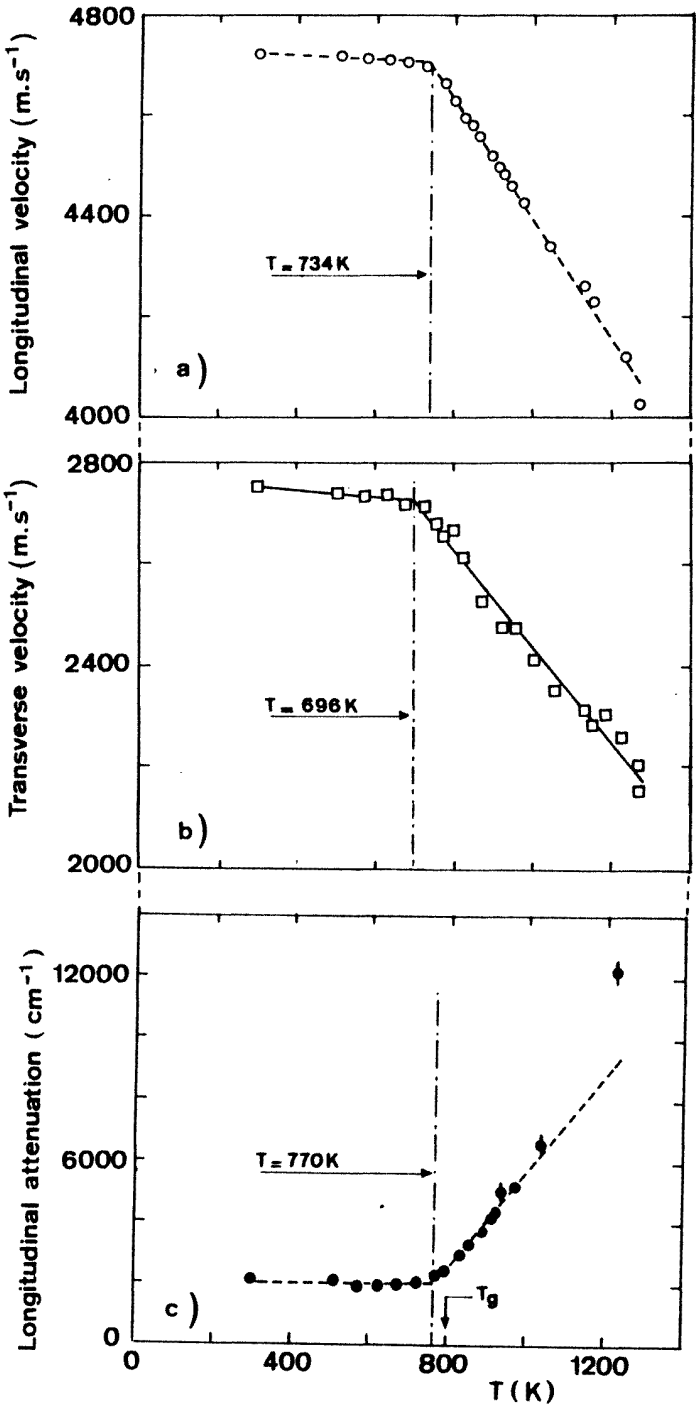

Figure 1. The hypersonic longitudinal velocity (a), transverse velocity (b), and longitudinal hypersonic attenuation (c) measured using Brillouin scattering as functions of temperature for BAF4. The solid and dashed lines are the results of linear regressions. The chain line indicates the intercept of the two lines corresponding to the low- and high-temperature regimes.

The longitudinal velocity of sound decreases with increasing temperature (figure 1(a)). The variations are very slow up to about 736 K and then a major break of slope indicates the glass transition temperature. As can be noticed in figure 1(b), the transverse velocity V_T follows the same behaviour as the longitudinal velocity V_L ($V_L \simeq V_T + 1970$ m s^{-1}). The break of slope of V_T is located at a slightly lower temperature (696 K) than that of V_L (73 K). The slopes $\mathrm{d}V_L/\mathrm{d}T$ and $\mathrm{d}V_T/\mathrm{d}T$ are similar within the experimental accuracy. However, for the comparison between the hypersound velocity and the position of the BP we will consider in section 3.2.2 the 'relative' slopes defined as $(\mathrm{d}V_L/\mathrm{d}T)(1/V_L)$ and $(\mathrm{d}V_T/\mathrm{d}T)(1/V_T)$.

The hypersonic longitudinal attenuation is nearly constant (within the experimental accuracy) up to 770 K, and then increases sharply by a factor of six when the temperature increases up to 1000 K (figure 1(c)). The transverse attenuation can be measured only in the right-angle scattering geometry, and is then polluted by a significant broadening due to the aperture of the collection lens. However, we noticed a break of slope at a temperature close to the glass transition temperature associated with a strong increase from 1000 cm^{-1} up to 400 K to 6000 cm^{-1} at 900 K.

3.2. Raman data

3.2.1. Normalization of the data. In order to eliminate the trivial temperature dependence, we always present in what follows spectra normalized to the Bose factor:

$$I_R(\omega, T) = \frac{I(\omega, T)}{\omega(n(\omega, T) + 1)} \qquad \text{for Stokes Raman intensity} \tag{1}$$

$$I_R(\omega, T) = \frac{I(\omega, T)}{\omega n(\omega, T)} \qquad \text{for anti-Stokes Raman spectra} \tag{2}$$

where $I(\omega, T)$ is the Raman intensity after subtracting the noise of the photo-multiplier, and $n(\omega, T)$ is the Bose factor. The temperature T can be slightly adjusted by taking into account the fact that the Stokes and anti-Stokes reduced intensities should be superimposed over the whole frequency range. This procedure gives a determination of the temperature in the sample. However, for the high-temperature measurements, the subtraction of the noise of the photo-multiplier was not sufficient for obtaining a good superposition, even if one allows large variations of the temperature parameter. An important frequency-dependent background due to thermal radiations emitted both by the oven and the sample is added to the Raman scattering. This contribution can be measured independently (without a laser beam) and fitted with a polynomial form which has been subtracted from the experimental intensity before reduction by the Bose factor. Then a satisfactory superposition of Stokes and anti-Stokes spectra was completed.

The reduced Raman intensities corresponding to various temperatures were normalized to one another using the integrated intensity in the 120–1000 cm^{-1} frequency range; the modes in this frequency range are temperature independent. Moreover, it has been checked that slight changes of the integration boundaries do not change the normalization factor. The normalized spectra are shown in figure 2. Note that the inset, on a log–log scale, reveals an approximate ω^{-1}-behaviour above the BP (50 cm^{-1}) as already observed in Raman scattering experiments performed on silica [30]. Buchenau explained such a behaviour observed via neutron scattering in polymers by considering a random symmetric dynamical matrix [8]: the application of Wigner's theorem to this matrix yields a constant density of eigenvalues, and then a density of states $g(\omega) \propto \omega$.

The neutron scattering signal is directly related to the vibrational density of states

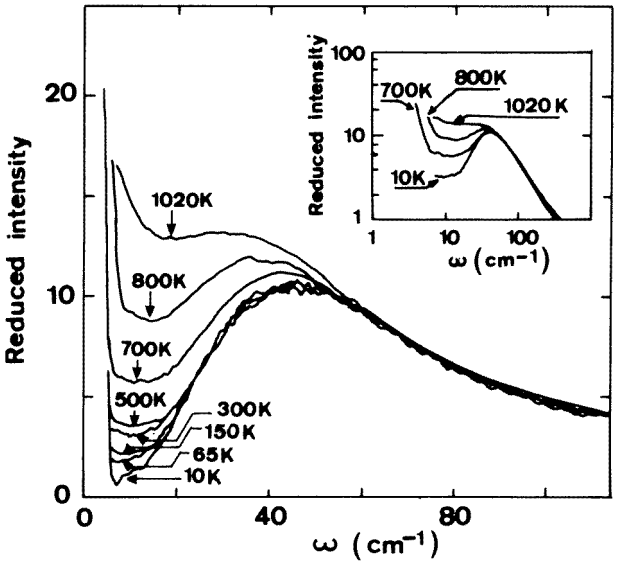

Figure 2. The reduced Raman intensity in arbitrary units for BAF4 from 10 to 1020 K normalized to the integrated intensity over the 120–1000 cm^{-1} range. The inset shows the approximate $1/\omega$ law after the BP.

(VDOS) whereas the Raman scattering introduces a coupling constant $C(\omega)$. Neutron scattering measurements on the same BAF4 sample presented over a limited range of frequency across the frequency of the maximum of the BP in reference [31] also show a similar law in ω^{-1} in the 33–66 cm^{-1} range. Therefore, if we extract a coupling constant $C(\omega)$ over the narrow frequency range, we find that it is frequency independent. This is a controversial and surprising result considering recent measurements on silica glasses based on the behaviour of $C(\omega)$ and its temperature dependence [33]. What we want to point out in this section is that the frequency dependence of this coupling constant remains an open question: it strongly depends on the frequency range in which the $\omega^{-\alpha}$-law for neutron scattering measurements of $g(\omega)/\omega^2$ is extracted (for silica $\alpha = 2$ [33] and $\alpha = 1$ [31] has been found, depending on the frequency range used for the determination of α). Thus, further investigations are needed at higher frequency, below and above the glass transition temperature, in order to give a conclusive determination of $C(\omega)$. Furthermore, the fact that the ω^{-1}-law has been found for fragile glass-forming liquids [8, 32] as well as for strong glass-formers suggests a universal law.

3.2.2. The boson peak. The VH Raman spectra for the BP frequency range (10–100 cm^{-1}) were analysed in the framework of two models which introduced relaxational and vibrational contributions.

The first model that we used, usually referred to as the 'superposition model' (SM) [19, 21], describes the vibrational and relaxation contributions by independent parameters. The BP is fitted either by a log–normal expression [20]:

$$I_R^{bp} = \frac{I_0^{bp}}{(2\pi\sigma^2)^{1/2}} \exp\left(-\frac{(\log\omega - \log\omega_{max})^2}{2\sigma^2}\right) \tag{3}$$

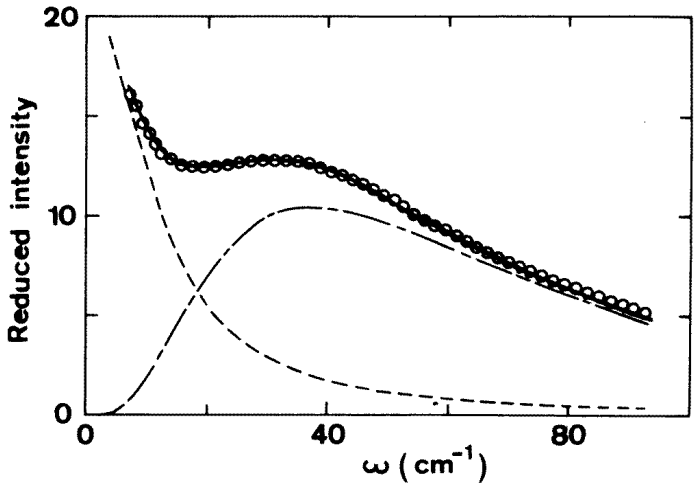

Figure 3. An example of the fitting procedure performed on the Raman spectra of BAF4 at 1020 K using the 'superposition model' (the fit is represented by the solid line). The vibrational contribution (chain line) is described by a log–normal function. The dashed line centred at zero frequency represents the relaxational contribution, and the circles are experimental data.

where I_0^{bp} is an amplitude factor, ω_{max} is the maximum of the BP, and σ is a parameter related to the width of the BP, or by a 'generalized Lorentzian' expression [21]:

$$I_R^{bp} = I_0^{bp}\omega^n \frac{1}{[\omega^2 + \omega_0^2]^m} \tag{4}$$

where I_0^{bp} is an amplitude factor, n and m are two exponents, and ω_0 is proportional to ω_{max}. This formula is a simplified version of that used in reference [21]. An additional relaxation contribution modelled by a Lorentzian contribution, centred on the laser line, has been taken into account [21]. This contribution introduces two extra parameters: the width and the amplitude of the Lorentzian. An example of such a fit using two independent vibrational and relaxational contributions is shown in figure 3. The fit of the relaxational contribution starts at about 10 cm^{-1}, since otherwise an elastic contribution could induce errors in the determination of the parameters. A good agreement is achieved over a large temperature range. However, for the lowest temperatures ($T < 300$ K) where the relaxation contribution is weak, the accuracy of the relaxation parameter is not very good. The position of the maximum of the BP ω_{max} deduced from such fits in the temperature range of the measurements is reported in figure 4. The values obtained in this way are compared to the position of ω_{max} without taking into account any relaxational contribution (i.e. the apparent position). The introduction of this latter contribution does not change the position of the BP at low temperature (below 600 K). Nevertheless, above 600 K the value of ω_{max} deduced from the SM is higher than the apparent position. The maximum effect is about 7–8 cm^{-1} at 1020 K. Thus the $d\omega_{max}/dT$ slope obtained by taking into account the relaxational contribution is lower than the apparent slope. The increasing values of ω_{max} below 600 K (figure 4) in the SM are not significant because in this temperature range the relaxational part is too weak to be accurately determined. Consequently, the variations are similar to those of the velocities (figure 1(a)): ω_{max} does not vary much up to about 600 K and then

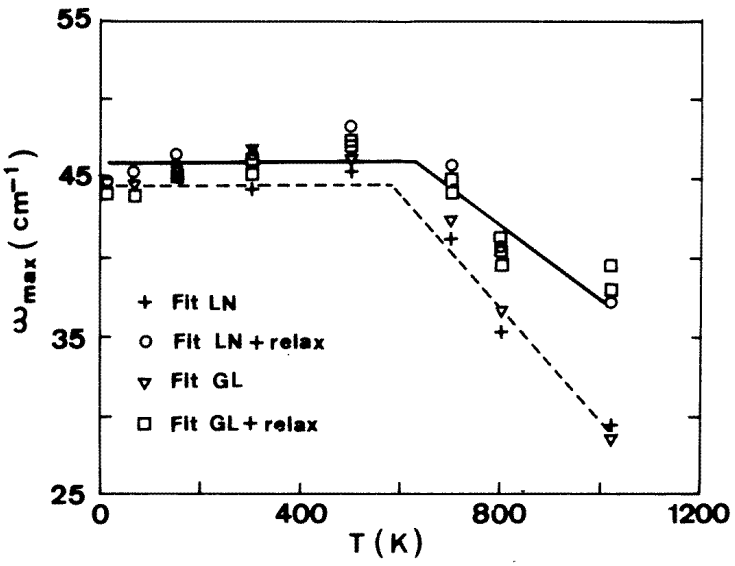

Figure 4. The positions of the maxima of the BP in BAF4 as functions of the temperature, determined by a simple superposition of a relaxational contribution (described by a Lorentzian) and a vibrational contribution described either by a log–normal (LN + relax = circle) or a generalized Lorentzian function (GL + relax = square). Also given is a comparison with the values of the apparent position of the maximum of the BP (without any relaxation contribution: LN = plus, GL = triangle). The solid and dashed lines are the results of linear regressions for the log–normal fits in both cases.

decreases strongly. However, the break of slope occurs at significantly lower temperature than that for the velocities.

Another recent study [6, 21, 34] considers correlations between relaxational and vibrational parts. The coupling introduces two parameters: the damping rate γ related to a relaxation time τ by $\gamma = 1/\tau$ and the coupling strength δ. This model, usually referred to as the 'coupling model' (CM), requires a measurement at low enough temperature to allow one to assume that the relaxational processes are frozen out for this temperature. This low-temperature spectrum is included as the vibrational contribution in the spectra at higher temperature. It has to be rescaled in frequency to account for the softening of vibrational modes as the temperature increases. The adjustable parameters are τ, δ, the position of the maximum of the vibrational contribution $\omega_{max}(T)$, and an amplitude factor I_0^{bp}. The Raman reduced intensity at a given temperature T is fitted to the following expression:

$$I_R(\omega, T) = \frac{1}{\omega} \int \frac{\mathrm{d}\Omega \; I_R^0(\Omega, T)\Omega^2\delta^2\omega\tau}{(\Omega^2 - \omega^2 - \delta^2)^2 + (\omega^2\tau^2(\Omega^2 - \omega^2)^2)} \tag{5}$$

where $I_R^0(\Omega, T)$ is the vibrational contribution deduced from the lowest-temperature (10 K) spectra. This expression is similar to that used in reference [6]. We used two different methods to determine $I_R^0(\Omega, T)$. Firstly, $I_R^0(\Omega, T)$ can be deduced from the experimental 10 K spectrum contracted along the frequency axis by the ratio of the adjustable variable $\omega_{max}(T)$ and the position of the BP at low temperature ω_{max}(10 K). Secondly, it can be

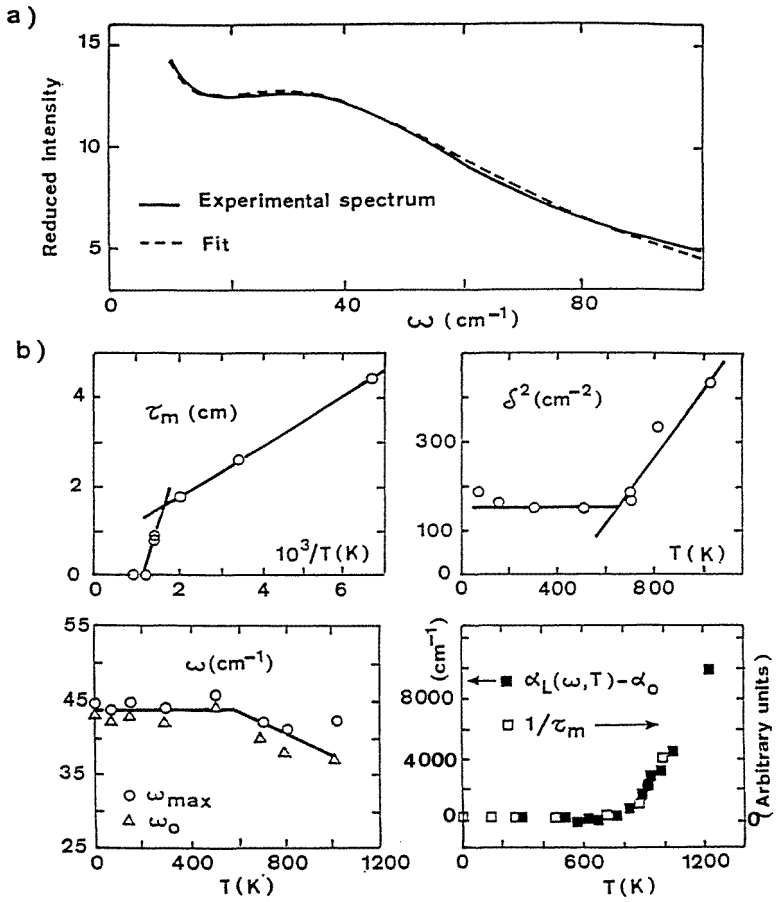

Figure 5. (a) An example of the best fit obtained using Gochiyaev's model. (b) The evolution with the temperature of the parameters $\tau_m = 2\omega_{max}^2\tau/\delta^2$ in cm, δ^2 in cm^{-2} and ω_{max} in cm^{-1} deduced from the fitting procedure. The variation with temperature of $1/\tau_m$ (cm^{-1}) on the one hand and the hypersonic attenuation $\alpha(\omega, T)$ (in cm^{-1}) subtracted from the low-temperature attenuation α_0 on the other hand are compared. The two quantities are proportional.

calculated using an analytical expression:

$$I_R^0(\omega, T) = I_0^{bp}\frac{\omega^n}{(\omega^2 + \omega_{max}(T)^2)^m} \tag{6}$$

where $\omega_{max}(T)$ is adjustable for each temperature, and n and m have been deduced by a fitting procedure from the lowest-temperature spectrum. Since the use of the experimental spectrum requires an interpolation with a very small step (10^{-2} cm^{-1}) to avoid the presence of oscillations when computing the integral, we used instead the second method which is less time consuming. A few examples of fitting procedures were performed with the two determinations of $I_R^0(\Omega, T)$ and led to the same parameters. An example of a fit is shown in figure 5(a), as well as the variations of the parameters δ^2, $\omega_{max}(T)$ and $\tau_m = 2\omega_{max}^2\tau/\delta^2$ deduced from the fitting procedure in figure 5(b). They are very similar to what was found for other glasses analysed using this model: a change of slope occurs for all parameters at a temperature close to T_g. As they were mainly fragile glasses [6, 21, 34], the present

work reveals a possible extension of this model toward strong glass-formers. Moreover, one can note that the lifetime of the vibration τ_m for frequencies around the BP can be related to the acoustic attenuation. This correlation can be seen in figure 5(b) which shows the similarity between the temperature dependence of τ_m and that of the Brillouin line width: $\tau_m \propto \alpha(\omega, T) - \alpha_0$ with $\alpha_0 \simeq 2000$ cm^{-1}. This relation has been established in the temperature range in which the parameters of the coupling model have significant meaning—i.e. above the glass transition temperature. We emphasize that this relationship cannot be extrapolated to the low-temperature regime. In the coupling model, the values $\omega_{max}(T)$ vary more slowly after the break of slope than in the superposition model.

Table 1. The quantitative correlation between the hypersonic velocity V and the position of the maximum of the boson peak ω_{max}. V_L and V_T represent the longitudinal and transverse velocities respectively. We compare the values at high temperature using two criteria: the position of the break of slope (B.S.) and the so-called 'relative' slopes $(\mathrm{d}V/\mathrm{d}T)(1/V(T_0))$ and $(\mathrm{d}\omega_{max}/\mathrm{d}T)(1/\omega_{max}(T_0))$ in K^{-1}, where T_0 is a value of temperature located after the break of slope for both quantities; we used $T_0 = 1000$ K. The position of the BP is determined from the apparent position, from the superposition model and from the coupling model. In the first two cases both log–normal and generalized Lorentzian forms have been used; the corresponding values are labelled as (LN) or (GL). When two values are reported for the same model, they correspond to different fitting ranges. The values of the break of slope are determined from the intercept of the two linear regressions performed within the low- and high-temperature regimes.

V			ω_{max}		
	$(\mathrm{d}V/\mathrm{d}T)(1/V(T_0))$	B.S.		$(\mathrm{d}\omega_{max}/\mathrm{d}T)(1/\omega_{max}(T_0))$	B.S.
V_L	-2.6×10^{-4}	734 K	Apparent position	-1.2×10^{-3} (LN)	580 K
				-1.4×10^{-3} (GL)	620 K
			Superposition model	$-(5\text{–}6) \times 10^{-4}$ (LN)	625 K
V_T	-3.9×10^{-4}	696 K		-4.9×10^{-4} (GL)	600 K
			Coupling model	-3.9×10^{-4}	570 K

The variations of $\omega_{max}(T)$ in the two models can be compared to the variation of the hypersonic velocity. In the low-temperature range (below the break of slope), the variations of the velocity of sound (figure 1(a), 1(b)) as well as the position of the maximum of the BP (figures 4 and 5(b)) are weak enough for us to consider that these physical quantities are constant within the accuracy of the experiments. In order to make a quantitative comparison at high temperature we have reported, in table 1, the position of the break of slope for the longitudinal and transverse velocities of sound and for ω_{max} deduced from the models presented above. We also calculated the values $(\mathrm{d}V/\mathrm{d}T)(1/V(T_0))$ and $(\mathrm{d}\omega_{max}/\mathrm{d}T)(1/\omega_{max}(T_0))$ where T_0 is a temperature above the breaks of slope, in the range of linear behaviour. These two ratios should be equal if V and ω_{max} are proportional. As we can notice from the second column of the table, the value of $(\mathrm{d}\omega_{max}/\mathrm{d}T)(1/\omega_{max}(T_0))$ decreases when a relaxational contribution is added, and further decreases if the coupling between the two contributions is taken into account. The value obtained is then close to that of $(\mathrm{d}V/\mathrm{d}T)(1/V(T_0))$. There is a qualitative correlation between the variation of ω_{max} in the coupling model and the velocity of sound in the VH and VV (vertical–vertical) polarizations. Nevertheless, a better agreement is obtained if one compares the transverse velocity of sound with the result of Gochiyaev's model.

As the Raman spectra are VH polarized, they are more sensitive to depolarized modes which probably originate from transverse acoustic modes. Moreover, we think that the

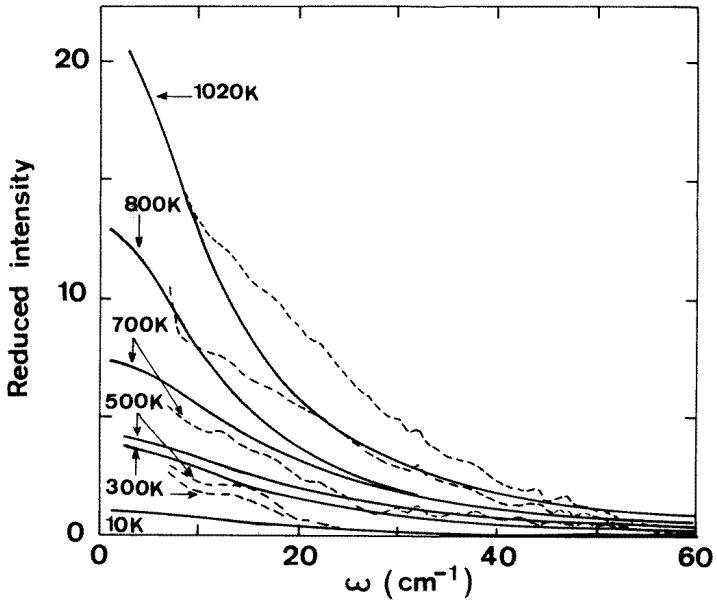

Figure 6. The relaxational contribution deduced from the fitting parameters of the Lorentzian simulating the relaxation in the superposition model (solid lines). The rough approximation obtained by subtracting the 10 K spectra from the current one (dashed line) without taking into account the softening of the vibrational contribution with increasing temperature is shown for comparison.

maximum of the vibrational density of states is dominated by the transverse modes, because in a crystal it is related to the Debye velocity which is dominated by the variations of the transverse modes.

3.2.3. The quasielastic intensity. In order to prove a correlation between the reduced Raman intensity and the hypersonic attenuation, we considered the total intensity or the relaxational intensity. The latter was determined by several methods:

(i) we used directly the values of the fitting parameters for the Lorentzian simulating the relaxation in the SM;

(ii) we subtracted an 'experimental' vibrational contribution determined from the low-temperature spectra, using the ratio of $\omega_{max}(10\ \mathrm{K})$ and $\omega_{max}(T)$ resulting from the SM or CM to account for the softening; and

(iii) we subtracted a similar experimental contribution where the softening was determined from the ratio of the velocities.

Independently of the model used for the analysis of the Raman spectra (superposition or coupling mode), we extracted an 'experimental' vibrational contribution using

$$I_R^{rel}(\omega, T) = I_R(\omega, T) - A I_R\left(\omega \frac{\omega_{max}(10\ \mathrm{K})}{\omega_{max}(T)}, 10\ \mathrm{K}\right) \tag{7}$$

where $\omega_{max}(T)$ and $\omega_{max}(10\ \mathrm{K})$ are the results from the fitting procedure with one of the two models; A is an amplitude factor adjusted so that the spectra are superimposed for frequencies above the maximum of the BP; and the low-temperature spectrum is assumed

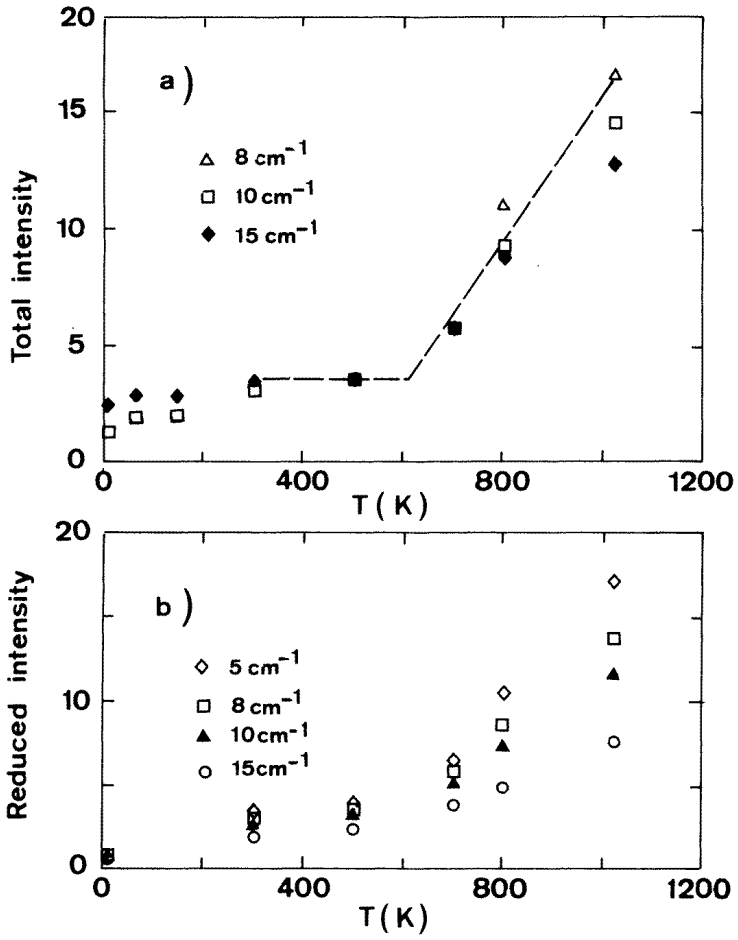

Figure 7. (a) The Raman reduced intensity as a function of the temperature for several frequencies. The dashed line is the result of a linear regression for 8 cm^{-1}. (b) The relaxational part of the Raman reduced intensity deduced from the superposition model as a function of the temperature.

to be vibrational only. As regards Gochiyaev's model, this method neglects the coupling between vibrations and relaxations. However, the result is comparable to the one obtained using the superposition model. The use of the ratio of the velocities relies on the assumption that $\omega(\omega, T) \propto V$.

An example of the relaxational contributions deduced from the fit using the SM is plotted in figure 6. In order to demonstrate the necessity of taking into account the softening of the vibrational contribution with increasing temperature, we also plotted the simple subtraction of the 10 K spectra from the current one. This latter method, which neglects the softening, is commonly used for extracting the relaxational contribution. The differences of the two curves in the 10 cm^{-1}–40 cm^{-1} region at each temperature range show the effect of the softening of the vibrational contribution. We checked that all of the methods described above give similar results.

It is then possible to compare the temperature dependence of the relaxational contribution

with the variations of the hypersonic attenuation. Though a comparison with the transverse attenuation would be more relevant, as pointed out in section 3.2.2, we used the longitudinal attenuation because it is determined with a much better accuracy. Figures 1(c) and 7(a), 7(b) show that the two physical quantities, i.e. longitudinal attenuation and Raman intensity, have very similar variations with temperature in the common range of the measurements (300–1200 K). The example in figure 7(b) concerns the relaxational contribution deduced for several frequencies from the fitting parameters of the Lorentzian simulating the quasielastic contribution in the SM. All of the methods produce similar temperature dependences.

Table 2. The quantitative correlation between the longitudinal hypersonic attenuation $\alpha_L(\omega, T)$ and the total or relaxational reduced Raman intensity $I_R(\omega, T)$ or $I_R^{rel}(\omega, T)$. We quote the same two criteria for $T > T_g$ and $T_0 = 1000$ K.

$\alpha(\omega, T)$			$I_R^{(rel)}(\omega, T)$		
	$(\mathrm{d}\alpha(\omega, T)/\mathrm{d}T)(1/\alpha(\omega, T_0))$	B.S.		$(\mathrm{d}I_R^{(rel)}(\omega, T)/\mathrm{d}T)(1/I_R^{(rel)}(\omega, T_0))$	B.S.
$\alpha_L(\omega, T)$	2.8×10^{-3}	770 K	Total intensity	1.9×10^{-3} (8 cm^{-1})	650 K
				1.7×10^{-3} (10 cm^{-1})	650 K
			Relaxational intensity(SM) (fits)	1.7×10^{-3} (1 cm^{-1})	600 K
				1.4×10^{-3} (15 cm^{-1})	620 K
			Relaxational intensity(SM) (experimental)	1.7×10^{-3} (8–15 cm^{-1})	550 K
			Relaxational intensity(CM) (experimental)	1.7×10^{-3} (8–15 cm^{-1})	550 K

We performed the same analysis as in section 3.2.2 in order to test for a correlation at high temperature between the Raman intensity and the hypersonic attenuation: the position of the break of slope for the longitudinal attenuation and for the Raman intensity as well as the values of $(\mathrm{d}\alpha(\omega, T)/\mathrm{d}T)(1/\alpha(\omega, T_0))$ and $(\mathrm{d}I_R^{(rel)}(\omega, T)/\mathrm{d}T)(1/I_R^{(rel)}(\omega, T_0))$ are reported in table 2 (in units of K^{-1}). As regards the Raman intensity, we have considered either the total intensity or the relaxational one. Between 300 K and 500 K the variations of the attenuation and of the Raman intensity are not significant. The two ratios defined above should be equal if $I_R^{(rel)}$ and α are proportional. Concerning the Raman intensity, $(\mathrm{d}I_R^{(rel)}(\omega, T)/\mathrm{d}T)(1/I_R^{(rel)}(\omega, T_0))$ has the same value (about 1.7×10^{-3} K^{-1}) if one considers the total intensity, the relaxational one deduced by subtracting the vibrational one in the framework of various models, and the relaxational contribution deduced from the fitting parameters (SM). These values have been determined for several frequencies ranging from 8 to 15 cm^{-1}. They are slightly increasing from 1.4×10^{-3} to 1.7×10^{-3} K^{-1} with decreasing frequencies.

The value of $(\mathrm{d}\alpha(\omega, T)/\mathrm{d}T)(1/\alpha(\omega, T_0))$ for the longitudinal attenuation, obtained by linear regression in the 800–1000 K range, is significantly higher: it is about 2.8×10^{-3} K^{-1}. The temperature dependence of $(\mathrm{d}I_R^{(rel)}(\omega, T)/\mathrm{d}T)(1/I_R^{(rel)}(\omega, T_0))$ is too weak to reach such a value at 1 cm^{-1}, which is the frequency of measurement of the longitudinal attenuation. The position of the break of slope (770 K) for the attenuation is also higher than the one for the Raman intensity (550–650 K). However, by analogy with the results found for the correlation between the hypersonic velocities and ω_{max}, we expect a better agreement with the transverse attenuation.

4. Discussion

We have presented in this paper Brillouin and Raman temperature-dependent measurements on a strong optical glass-former. The purpose of this work was to establish correlations between the Brillouin results (the attenuation and velocity) and the Raman characteristics (the reduced intensity and the position of the BP). Therefore, we considered several models yielding different methods to extract the relaxational and vibrational contributions in the Raman spectra and thus the position of the BP.

For the first correlation, very few experimental proofs of the relationship of proportionality between the reduced Raman intensity and the sound wave attenuation in the GHz range are available. In fact, this evidence requires measurements of the hypersonic attenuation α via Brillouin scattering data using a high-resolution spectrometer. Moreover, α can be extracted only at the frequency of the Brillouin shift. An attempt to calculate the hypersonic attenuation using a model of relaxation defects and parameters extracted from ultrasonic measurements data failed because of additional contributions to the attenuation due to anharmonicity, or to the existence of defects at hypersonic frequencies inefficient at ultrasonic frequencies [35]. Although a recent study establishes that the temperature and frequency dependence of the quasielastic scattering agrees qualitatively with the predictions of the soft-potential model (i.e. a proportionality with the hypersonic attenuation), more significant comparison using experimental data for the attenuation is still needed [36]. Such a comparison was tested for boron oxide glass as a function of temperature (from 20 K to the glass transition temperature $T_g = 540$ K): a good connection was found below 300 K only, and could not be extended to glasses of different composition (B_2O_3–$x$$Li_2O$) [37]. A recent attempt to check whether the connection holds for several samples was successfully performed at room temperature on silica samples [30]. The reduced Raman intensity and the hypersonic attenuation have clearly correlated variations for various silica samples: a linear relation was found between these two quantities for samples with different OH contents, different fictive temperatures, and irradiated crystalline quartz and vitreous silica. The connection is better if one considers the relaxational part only. In both cases the linear law intercepts the attenuation axis at a nonzero value: the hypersonic attenuation has a finite value when the Raman intensity is extrapolated to zero. This can be explained by the existence of contributions to the attenuation of frozen-in fluctuations or geometrical scattering of sound which do not contribute to the quasielastic intensity. A qualitative agreement (i.e. a similar increase with fictive temperature for the Raman intensity and the hypersonic attenuation) was obtained for barium-crown dense glasses with different fictive temperatures [27, 38].

In this paper, we found clear evidence for such a correlation for a BAF4 (Schott) strong glass as a function of the temperature in the 300–1000 K range. All of the reduced Raman intensities, either total or relaxational, deduced by any of the methods mentioned above, are correlated with the longitudinal hypersonic attenuation. In the temperature range in which the transverse attenuation has been accurately determined, its temperature dependence is also connected with that of the Raman intensity. Since the total reduced intensity and the relaxational part are correlated to the same extent with the variation of the hypersonic attenuation, it is difficult to decide whether one relationship of proportionality is better than the other. To clarify this ambiguity, measurements carried out at lower frequencies near the central line, on a high-resolution Raman spectrometer, will allow a more precise determination of the quasielastic contributions. Moreover, further investigations are planned at temperatures well above T_g in the liquid state (up to 1600 K) using a high-temperature furnace. In this temperature range, we expect that the transverse modes will be over-

damped; thus it will be possible to elucidate whether the correlation gives better results with the transverse attenuation.

For the second correlation, as pointed out in the introduction, it has often been mentioned that the position of the BP varies proportionally to the velocity of sound [40, 39]. Nevertheless, most studies make use of the apparent position of the BP. Indeed, few works present models including relaxations and vibrations, or a comparison of several models for determining the position of the maximum of the BP ω_{max}. Krüger *et al* saw very similar variations of the position of the BP maximum determined using the superposition model on the one hand and Gochiyaev's coupling model on the other hand [21]. The only difference was the temperature at which ω_{max} is no longer constant: this temperature is equal to T_g if one uses the coupling model instead of being higher than T_g as it is if one uses the SM. Similarly, we found ω_{max} constant up to a lower temperature in the case of the CM; thus the break of slope is then closer to that of the hypersonic velocity. For the values of $(\mathrm{d}\omega_{max}/\mathrm{d}T)(1/\omega_{max}(T_0))$, a clear quantitative agreement is obtained if one determines ω_{max} from the CM, whereas the relationship of proportionality is not well fulfilled if the coupling between relaxational and vibrational contributions is not taken into account: the values of the slopes are about four times too high if one considers the apparent position of the BP, twice too high for the SM. The agreement in the case of the CM is more relevant for the transverse velocity. Hitherto, most of the comparisons have been undertaken between ω_{max} and the longitudinal velocity. In a glass-forming liquid ortho-terphenyl a partial correlation between the BP and the transverse velocity was found only on the basis of their simultaneous disappearance at about $1.3T_g$ and qualitatively similar variations [39]. Another investigation carried out on B_2O_3 [40], considered the average velocity of sound $V_a = (V_L + 2V_T)/3$, where V_T and V_L are the transverse and longitudinal velocities respectively, and discussed the close correspondence between the hypersonic velocity and the low-frequency vibrational behaviour (the BP). However, these analyses led neither to a quantitative relationship nor to reliable evidence. In this paper, we emphasize that the transverse velocity is more suitable for proving this correlation.

5. Conclusion

We have presented a detailed study of Raman and Brillouin scattering measurements for a strong glass over a broad range of temperatures. Our purpose was to investigate whether the low-frequency vibrational behaviour is correlated with the elastic properties. Many attempts have been made previously to achieve this aim for fragile and intermediate glasses. However, the connection remains unclear, and no theory can quantitatively account for it. Several interpolation formulas and schematic models have been proposed to describe the Raman spectra, but none of these has been subjected to rigorous experimental tests. In this work we insist on a careful comparison of the models in order to demonstrate that more attention must be devoted to both the evaluation of the quasielastic contribution and the determination of the position of the boson peak, which are crucial points in determining the reliability of the theoretical predictions. Indeed, we point out that the decrease of the boson peak frequency above the break of slope depends on the approach used for the extraction of the vibrational modes. The variations can be either equal to or faster than the variation of the velocity of sound, depending on whether the relaxational part has been taken into account or not. A careful analysis leads to a convincing correlation between the position of the boson peak and the hypersonic velocity in both polarizations; in particular the connection is slightly better if one considers the transverse velocity. Another important underlying result in this paper is the fact that the correlation between the quasielastic Raman intensity and the

hypersonic attenuation is fulfilled by varying the temperature over a broad range across T_g. To sum up, we have demonstrated a strong correlation between the Raman features (at a few tens of cm^{-1}) and the Brillouin data (at 1 cm^{-1}) suggesting that the same mechanism is responsible for the vibrational dynamics within the 1–50 cm^{-1} range. This supports the idea that the modes responsible for the boson peak have the same origin as the acoustic phonons, and that the attenuation of phonons is due to an interaction with defects responsible for the quasielastic intensity. Moreover, the behaviour of the position of the boson peak shows a break of slope clearly below the change of slope for the transverse velocity, itself located at a temperature lower than the glass transition temperature T_g; this is the case for all of the models used in this study. This means that the high-frequency acoustical modes soften at lower temperature than the low-frequency modes. This result goes against former studies for fragile materials, where the break of slope occurs at T_g [40, 41].

Another relevant point stressed in this paper is that a pronounced softening of the boson peak occurs as an increase of the quasielastic intensity sets in (at 600 K) far below the glass transition temperature ($T_g \simeq 800$ K). This feature is consistent with recent experiments on fragile glasses, and demonstrates that even for oxide glasses a quasielastic contribution due to a fast relaxation is observed [7]. This indicates a coexistence of vibrational and relaxational modes, and suggests that the same underlying physics is responsible for the two features of the Raman spectra. This result is in accordance with the recent theoretical explanation in terms of low-barrier structural relaxations arising from vibrational modes localized within a double-well potential.

Acknowledgments

We are very grateful to Professor U Buchenau for encouraging us at the start of this study. We also thank Professor D Quitmann for fruitful discussions and Dr Ph Jund for a critical reading.

References

[1] Götze W and Sjögren L 1992 *Rep. Prog. Phys.* **55** 241
[2] Götze W and Sjögren L 1988 *J. Phys. C: Solid State Phys.* **21** 3407
[3] Angell C A 1984 *Relaxation in Complex Systems* ed K L Ngai and G B Wright (Washington, DC: Office of Naval Research) p 3
[4] Sokolov A P, Rössler E, Kisliuk A and Quitmann D 1993 *Phys. Rev. Lett.* **71** 2062
[5] Rössler E, Sokolov A P, Kisliuk A and Quitmann D 1994 *Phys. Rev.* B **49** 14 967
[6] Gochiyaev V Z, Malinovsky V K, Novikov V N and Sokolov A P 1991 *Phil. Mag.* B **63** 777
[7] Buchenau U, Schönfield C, Richter D, Kanaya T, Kaji K and Wehrmann R 1994 *Phys. Rev. Lett.* **73** 2344
[8] Buchenau U 1995 *Phil. Mag.* **71** 793
[9] Karpov V G, Klinger M I and Ignat'ev F N 1983 *Sov. Phys.–JETP* **57** 439
[10] Il'in M A, Karpov V G and Parshin D A 1987 *Sov. Phys.–JETP* **65** 439
[11] Pang T 1992 *Phys. Rev.* B **45** 2490
[12] Duval E, Boukenter A and Achibat T 1990 *J. Phys.: Condens. Matter* **2** 10 227
[13] Phillips J C 1981 *J. Non-Cryst. Solids* **431** 37
[14] Elliot S R 1992 *Europhys. Lett* **19** 201
[15] Akkermans E and Maynard R 1985 *Phys. Rev.* B **32** 7850
[16] Schirmacher W and Wagener M 1993 *Solid State Commun.* **86** 597
[17] Klinger M I 1992 *Phys. Lett.* **170A** 222
[18] Martin A and Brenig W 1974 *Phys. Status Solidi* b **64** 163
[19] Malinovski V K and Sokolov A P 1986 *Solid State Commun.* **57** 757
[20] Malinovsky V K, Novikov V N and Sokolov A P 1991 *Phys. Lett.* **153A** 63
[21] Krüger M, Soltwisch M, Petscherizin I and Quitmann D 1992 *J. Chem. Phys.* **96** 7352

[22] Jäckle J 1981 *Amorphous Solids. Low-Temperature Properties (Springer Topics in Current Physics 24)* ed W A Phillips (Berlin: Springer)
[23] Theodorakopoulos N and Jäckle J 1976 *Phys. Rev.* B **14** 2637
[24] Gurevich V L, Parshin D A, Pelous J and Schober H R 1993 *Phys. Rev.* B **48** 16 318
[25] Parshin D A 1994 *Phys. Solid State* **36** 991
[26] Buchenau U, Zhou H M, Nucker N, Gilroy K S and Phillips W A 1988 *Phys. Rev. Lett.* **60** 1318
[27] Vacher R, Delsanti M, Pelous J, Cecchi L, Winter A and Zarzycki J 1982 *J. Mater. Sci.* **9** 829
[28] Scholtze H 1974 *Le Verre, Nature, Structure et Propriétés* (Paris: Institut du Verre)
[29] Winter A 1943 *J. Am. Ceram. Soc.* **26** 189
[30] Terki F, Levelut C, Boissier M and Pelous J 1996 *Phys. Rev.* B **53** 2411
[31] Buchenau U 1993 *Physica* A **201** 372
[32] Wuttke J, Petry W, Coddens G and Fujara F 1995 *Phys. Rev.* E **52** 4026
[33] Sokolov A, Buchenau U, Steffen W, Frick B and Wischnewski A 1995 *Phys. Rev.* B **52** R9815
[34] Sokolov A P, Kisliuk A, Quitmann D, Kudlik A and Rössler E 1994 *J. Non-Cryst. Solids* **172–174** 138
[35] Berret J F, Pelous J, Vacher R, Raychaudhuri A K and Schmidt M 1986 *J. Non-Cryst. Solids* **87** 70
[36] Brodin A, Fontana A, Börjesson L, Carini G and Torell L M 1994 *Phys. Rev. Lett.* **73** 2067
[37] Lörosch J, Couzi M, Pelous J, Vacher R and Levasseur A 1984 *J. Non-Cryst. Solids* **69** 1
[38] Levelut C, Gaimes N, Terki F, Cohen-Solal G, Pelous J and Vacher R 1995 *Phys. Rev.* B **51** 8606
[39] Steffen W, Zimmer B, Patkowski A, Meier G and Fischer E W 1994 *J. Non-Cryst. Solids* **172–174** 37
[40] Hassan A K, Torell L M and Börjesson L 1992 *J. Physique* IV C2 265
[41] Hassan A K, Börjesson L and Torell L M 1994 *J. Non-Cryst. Solids* **172–174** 154